Measurement of Heart Rate Variability Using an Oscillometric Blood Pressure Monitor

Saif Ahmad, Miodrag Bolic, *Senior Member, IEEE*, Hilmi Dajani, *Member, IEEE*, Voicu Groza, *Senior Member, IEEE*, Izmail Batkin, and Sreeraman Rajan, *Senior Member, IEEE*

Abstract—We apply the maximal overlap discrete wavelet transform (MODWT)-based spectral density estimation method to measure heart rate variability (HRV) from short-duration pulse wave signals produced by an automated oscillometric blood pressure (BP) monitor during routine measurements. To test the accuracy of this wavelet HRV metric, we study the linear correlations that it achieves with chronological age and BP in a healthy population of 85 subjects. We define accuracy as the quality of the linear regression of HRV with age and BP. Results are compared with a number of traditional HRV metrics and earlier published work. The MODWT HRV metric achieves higher (and more significant) correlations with age and BP compared to other metrics. Moreover, these correlations are in agreement with earlier published work on correlations of HRV (measured from much longer duration electrocardiogram signals) with age and BP. As a further enhancement, we combine the MODWT HRV metric with other HRV metrics inside a multiple-linear-regression model and show an improvement in the correlations between the predicted and actual ages and the predicted and actual BP. Our work thus indicates the suitability of the MODWT metric either as a stand alone or in combination with other metrics for characterizing HRV from short-duration oscillometric pulse wave signals. Based on our results, we conclude that oscillometric BP monitors can be used to measure HRV in addition to measuring BP.

Index Terms—Electrocardiogram (ECG), heart rate variability (HRV), oscillometric blood pressure (BP), pulse wave signal, wavelet spectral density, wrist monitor.

I. INTRODUCTION

HEART rate variability (HRV), a measure of the beat-to-beat fluctuations in the heart rate (HR), is an important biomarker of health and illness [1]. HRV is computed by analyzing beat-to-beat interval time series derived from an electrocardiogram (ECG), an arterial pressure tracing, or a plethysmographic pulse wave signal. A variety of metrics have been proposed for measuring HRV. These metrics can broadly be classified into time- [2], frequency- [3], complexity- [4], fractal- [5], and nonlinear- [6] domain measures of HRV.

Alterations—generally reductions—in HRV have been found to be diagnostic and prognostic of pathologic states such as hypertension [7]–[9], heart failure [10], [11], and septic shock [12], [13]. HRV has been found to be augmented in the physically fit [14] and has been shown to diminish with age [15]–[19]. Most studies have reported the degree of alteration in HRV to be correlated with the severity of the pathology.

In the last decade or so, wavelet-based time–frequency analysis has received much attention for characterizing HRV from ECG signals. Lin *et al.* employed thresholds based on the amplitude characteristics of wavelet decompositions of HRV signals to discriminate between healthy and congestive heart failure subjects [20]. In a similar study, Thurner *et al.* used the wavelet decomposition standard deviation to classify patients as normal or with congestive heart failure [21]. Ivanov *et al.* studied power law behavior in probability distributions of wavelet decompositions of HRV signals [22]. They found scale-invariant power law behavior in wavelet probability distributions of normal subjects, whereas such behavior was absent in subjects who suffer from sleep apnea. Verlinde *et al.* measured the average power (amplitude) of wavelet decompositions of HRV signals in controls and aerobic athletes [23]. Their results revealed that the average power of wavelet decompositions in all frequency bands was higher for aerobic athletes as compared to controls.

Since HRV information may either be extracted from ECG or pulse wave signals, many studies have assessed the differences between the two. While some studies have shown good agreement between ECG and pulse-wave-based HRV [24], [25], others have shown that the latter is not a surrogate for the former [26].

Despite an abundance of literature on HRV analysis and its usefulness in assessing physiological status, no study, to the best of our knowledge, reports the analysis of short-duration pulse wave signals produced by oscillometric blood pressure (BP) monitors. Moreover, no published work reports characterization of HRV from ECG and/or pulse wave signals of durations shorter than 180 s. This may be attributed to the recommendations of the task force of the European Society of Cardiology and the North American Society of Pacing and Electrophysiology [27]. This task force recommends that all short-term HRV analysis should be carried out on signals that are 300 s long, while all long-term HRV analysis should be carried out on signals that are 86 400 s long. However, the pulse wave signals produced by automated oscillometric BP monitors generally have a duration range of 30–90 s—the time taken by these monitors to complete a routine measurement. Therefore, these short- and variable-duration HRV signals produced by

an oscillometric BP monitor present a challenge for accurate characterization of HRV.

In this paper, we introduce a new approach of measuring HRV from short- and variable-duration (31–95 s) pulse wave signals produced by an automated oscillometric BP monitor during routine measurements. To characterize HRV, we employ the maximal overlap discrete wavelet transform (MODWT)-based spectral density estimation method introduced by Percival and Walden [28]. Preliminary results of this research were presented in [29], wherein the accuracy of the MODWT HRV metric was evaluated by studying its linear correlations with chronological age and mean arterial pressure (MAP) in a healthy population of 85 subjects. We defined accuracy as the quality of the linear regression of HRV with age and BP. The correlations achieved by the MODWT metric were compared with those achieved by other HRV metrics, i.e., standard deviation (SD), root mean square successive difference (RMSSD), fast Fourier transform (FFT), sample entropy (SampEn), and earlier published work. The MODWT HRV metric achieved higher and more significant correlations with age and MAP compared to other metrics. Moreover, these results were in agreement with earlier published work on correlations of HRV (measured from much longer duration ECG signals) with age and BP. Our results thus showed that the MODWT HRV metric offers an effective means of accurately measuring HRV from short- and variable-duration pulse wave signals produced by an oscillometric BP monitor during routine measurements [29].

Here, we extend the work presented in [29] by: 1) incorporating more HRV metrics (fractal domain detrended fluctuation analysis (DFA) and nonlinear domain Poincaré plot analysis) in our analysis to enable the comparison of the MODWT HRV metric with a wider range of alternative HRV measures, 2) including systolic and diastolic BP in addition to MAP for studying HRV and BP correlations more comprehensively, 3) undertaking a correlation analysis amongst all HRV metrics to understand the relationships between them, 4) performing a multiple linear regression analysis utilizing combinations of various HRV metrics to assess if correlations between the predicted and actual age, and the predicted and actual BP can be improved in comparison to single regression, and 5) comparing our results with a larger body of published work on much longer and constant duration ECG signals to highlight the effectiveness of the proposed approach.

The MODWT metric achieves higher (and more significant) correlations with age and BP compared to all other metrics, and our results conform to earlier published work. Multiple-regression modeling, which combines the MODWT metric with other metrics, improves correlations between the predicted and actual ages and the predicted and actual BP. These results suggest that multiple measures provide a more comprehensive characterization of HRV compared to single measures. Thus, our work indicates the suitability of the MODWT metric either as a stand alone or in combination with other metrics for characterizing HRV from short duration oscillometric pulse wave signals. From our results, we conclude that oscillometric BP monitors can be used for measuring HRV in addition to measuring BP.

II. METHODS

A. Participants

Eighty five healthy subjects ($N_T = 85$; age range: 12–80 yrs), 37 of whom were females ($N_F = 37$; age range: 17–65 yrs) and 48 were males ($N_M = 48$; age range: 12–80 yrs), participated in the study. No subjects had any history of cardiovascular or respiratory disease, to the best of our knowledge. The local ethics committee approved the study, and written informed consent was obtained before enrolling participants in the study.

B. Data Collection

Pulse wave signals were acquired using an automated oscillometric wrist BP monitor (UFIT ® TEN-10, Biosign Technologies Inc., Toronto, ON, Canada) at a sampling rate of 100 Hz.

The American Heart Association (AHA) committee [30] and the task force of the European Society of Cardiology and the North American Society of Pacing and Electrophysiology [27] recommend that an ECG sampling frequency range of 250–500 Hz is optimum for accurate characterization of HRV. Nonetheless, studies that specifically investigated the effects of ECG sampling rate on the accuracy of HRV analysis found that sampling frequencies as low as 100 Hz offer equivalent fidelity to that offered by higher sampling frequencies (300–500 Hz) [31]–[33]. Moreover, investigators have successfully extracted useful physiologic information from HRV analysis performed on ECG signals sampled at around 100 Hz [34], [35].

No guidelines currently exist regarding the ideal sampling frequency of pulse wave signals for HRV characterization. In addition, no studies have investigated the relationship between the sampling frequency of pulse wave signals and the accuracy of HRV analysis. However, given the typical frequency spectrum of pulse peaks (1–15 Hz) [36], [37], it follows from the Shannon sampling theorem [38] that a sampling frequency of 100 Hz is sufficient to provide correct estimation of HRV. That is, pulse wave signals sampled at frequencies higher than 100 Hz would not provide any additional information. Indeed, a survey of relevant literature also suggests that HRV can be assessed efficiently from pulse wave signals sampled at around 100 Hz [37], [39].

Therefore, from the above discussion, we conclude that HRV can be accurately measured from the oscillometric pulse wave signals produced by the UFIT ® BP monitor at a sampling rate of 100 Hz.

The UFIT ® TEN-10 wrist BP monitor is a portable electronic unit that connects to a personal computer (PC) through a universal serial bus (USB) connector. The device is powered by the user's computer. It has a PC-based user interface, which is used to initiate a measurement. Once a measurement is complete, the interface prompts the user to log in and process the measurement. When the user enters his or her login information and hits the process button, the collected data is transferred to the Biosign web server (over an ordinary Internet connection), where it is processed using proprietary software. The processed data, i.e., the cuff pressure waveform, the derivative of the cuff pressure waveform, and the systolic and diastolic BP values, is returned to the user's PC in a format of their choosing. The data

transfer (back and forth) and processing take approximately 3 s. We used the derivative of the cuff pressure waveform to measure HRV by employing software that we developed in Matlab $\circledR$ R2006a (The MathWorks Inc., Natick, MA, USA).

The choice of the UFIT $\circledR$ automated oscillometric wrist BP monitor for this study was based on two factors. First, it conveniently interfaces with a PC to provide seamless data transfer. Second, automated wrist BP monitors have now become a standard in BP monitoring and are being widely and successfully used around the world.

Each collected pulse wave signal was produced by the UFIT $\circledR$ TEN-10 BP monitor during the period that it measured systolic and diastolic BP. Five signals each $\{\text{UFIT}_k | k = 1, \ldots, 5\}$ were collected from 84 subjects, and four signals $\{\text{UFIT}_k | k = 1, \ldots, 4\}$ were collected from one subject, resulting in a total of 424 oscillometric BP signals (duration range: 31–95 s, duration median: 55 s). The variation in duration (31–95 s) of the pulse wave signals acquired by the UFIT $\circledR$ BP monitor can be explained as follows. The monitor establishes a rough estimate of a subject's systolic and diastolic BP before initiating a measurement or the process of inflation and deflation of the cuff. For example, for a subject whose BP is estimated to be high by the monitor, it inflates the cuff to a desired higher pressure. Hence, the resulting oscillometric signal duration is longer, because it takes the monitor longer to deflate the cuff back to zero pressure from this higher starting pressure. Therefore, the variation in duration (31–95 s) of the pulse wave signals acquired by the UFIT $\circledR$ BP monitor resulted from the different initial BP estimates that the monitor made from subject to subject for 85 subjects ($N_T = 85$). We had no control over the durations of the signals acquired by the UFIT $\circledR$ monitor.

The aim of this study was not to validate the UFIT $\circledR$ automated wrist BP monitor with a classic upper arm sphygmomanometer. However, as per the SP10 BP measurement standards [40], for each of the 424 pulse wave signals acquired by the UFIT $\circledR$ automated wrist BP monitor, we collected analogous systolic and diastolic BP values employing the classic auscultatory brachial BP measurement method. This approach was adopted for two reasons: 1) to validate the systolic and diastolic BP values produced by the UFIT $\circledR$ automated wrist BP monitor in the future (if required) and 2) to correlate HRV measured from pulse wave signals produced by the UFIT $\circledR$ automated wrist BP monitor with analogous classic auscultatory brachial BP measurements for this study.

Because of the problem of occlusion of brachial arteries by upper arm sphygmomanometers, simultaneous brachial and wrist measurements were not possible. Therefore, approximately 1.5 min after each pulse wave signal acquisition by the UFIT $\circledR$ automated wrist BP monitor, two nurses simultaneously recorded systolic (SP_1 and SP_2) and diastolic (DP_1 and DP_2) BP using a classic upper arm sphygmomanometer provided with means for simultaneous readings. Readings with subscript 1 were taken by nurse 1, and readings with subscript 2 were taken by nurse 2. This resulted in five pairs of systolic $\{SP_{1,k}, SP_{2,k}, | k = 1, \ldots, 5\}$ and diastolic $\{DP_{1,k}, DP_{2,k}, | k = 1, \ldots, 5\}$ BP values for each subject—five measured by nurse 1 $\{SP_{1,k}, DP_{1,k}, | k = 1, \ldots, 5\}$ and five measured by nurse 2 $\{SP_{2,k}, DP_{2,k}, | k = 1, \ldots, 5\}$.

Thus, each of the five classic BP measurements taken by nurses 1 and 2 $\{(SP_{1,k}, SP_{2,k}), (DP_{1,k}, DP_{2,k}), | k = 1, \ldots, 5\}$ corresponded with a delay of about 1.5 min to each of the five pulse wave signals recorded by the automated oscillometric BP monitor $\{\text{UFIT}_k | k = 1, \ldots, 5\}$ for each subject. This delay between the arm and wrist measurements should be not only as short as possible to minimize the natural BP variation in time but also long enough to let the system settle down after the occlusion of arteries during measurements. The 1.5-min delay between arm and wrist measurements is a compromise that aims at minimizing the method errors [40].

In this study, we used the HRV measured from pulse wave signals produced by the UFIT $\circledR$ automated wrist BP monitor to correlate with analogous classic auscultatory brachial BP measurements recorded by the nurses and with subject age.

C. Deriving HRV Signals

The oscillometric pulse wave signals were cleaned using bandpass filtering. The cut-off frequencies for the bandpass filter were kept at 0.5 and 20 Hz. The bandpass filtering did not change the relative temporal positions of pulse peaks (or HRV information) in the filtered signal, because the choice of the frequency spectrum of the bandpass filter (0.5–20 Hz) ensured that it accommodated the frequency spectrum of typical pulse peaks (1–15 Hz) [36], [37]. The bandpass filtering was followed by the identification of pulse peaks by employing a local maxima detection algorithm.

All data was visually inspected and manually corrected for any peaks that were falsely identified or missed by the peak detection algorithm. For all subjects ($N_T = 85$), out of a total of 29 626 true peaks, 911 (3%) were either falsely identified or missed by the peak detection algorithm. Given the short durations (31–95 s) of our signals, we chose to manually correct all falsely identified or missing peaks to maximize the accuracy of our analyses. The manual peak correction exercise was straightforward and unambiguous, because signal durations were short, and all true peaks were clearly visible for each signal.

Finally, based on the identified pulse peaks, we derived the pulse-to-pulse (PP) interval time series (HRV signals).

D. Wavelet and Other HRV Metrics

Wavelet analysis provides a simultaneous time and frequency (or timescale) representation of a signal. Unlike the Fourier analysis, which only measures the overall frequency content of a signal [41], wavelet analysis provides a temporal resolution of the spectral content of a signal [42]. This makes the wavelet analysis an attractive tool for studying signals that are characterized by nonstationarity, noise, and local transients.

We employed the MODWT [28] using Mallat's pyramidal decomposition paradigm [43] to analyze the HRV signals. Daubechies least asymmetric 8-tap (LA8) filters [44] were used for the computation of the MODWT. The MODWT algorithm that we employed is presented in Fig. 1, where X is the input HRV signal with N number of samples, and H_j and G_j are the high- and low-pass filters, respectively, with M taps or coefficients ($M = 8$, for $j = 1$). The HRV signal X is symmetrically

1. The HRV signal, $X = [x_0, x_1, ..., x_{(N-1)}]$, which has N samples, is symmetrically extended by mirroring its samples. The signal is mirrored by $2N$ samples to the left and by $2N$ samples to the right, resulting in a total of $5N$ samples. Mathematically,

$$Y = [X \ X.F \ X \ X.F \ X],$$

where F is a $N \times N$ matrix whose entries are given by,

$$F_{a,b} = 1, \ \text{if} \ \{(a + b - 1) = N\},$$

$$= 0, \text{otherwise}.$$

2. The mirrored HRV signal, $Y = [y_0, y_1, ..., y_{(5N-1)}]$, which has $5N$ samples, is convolved with the level $j = 1$ MODWT high-pass filter, $H_1 = [h_{1,0}, h_{1,1}, ..., h_{1,(M-1)}]$, which has M filter coefficients, to obtain a convolution vector, P_1,

$$P_1 = (H_1 * Y) = \left\{ P_1[i] = \sum_{q=0}^{M-1} H_1[q] \, Y[i - q], i = 0, 1, 2, ..., (5N + M - 2) \right\},$$

where * denotes the convolution operation. That is, the convolution vector, $P_1 = [p_{1,0}, p_{1,1}, ..., p_{1,(5N+M-2)}]$, has $(5N + M - 1)$ samples.

3. The level $j = 1$ MODWT wavelet coefficients, W_1, are obtained by selecting samples from indices $2N$ to $(4N - 1)$ from the convolution vector P_1. That is,

$$W_1[i] = P_1[i], \ \text{for} \ \{2N \le i \le (4N - 1)\}.$$

Thus, the wavelet coefficients, $W_1 = [w_{1,0}, w_{1,1} ..., w_{1,(2N-1)}] = [p_{1, 2N}, p_{1, (2N+1)}, ..., p_{1, (4N-1)}]$, have $2N$ samples.

4. The mirrored HRV signal, Y, is convolved with level $j = 1$ MODWT low-pass filter, G_1, which has M filter coefficients, to obtain the convolution vector (similar to Step 2). The level $j = 1$ MODWT scaling coefficients, V_1, are obtained by selecting samples from indices $2N$ to $(4N - 1)$ from the convolution vector (similar to Step 3). Thus, the scaling coefficients, V_1, have $2N$ samples.

5. The level $j = 1$ MODWT high-pass (H_1) and low-pass (G_1) filters are rescaled or up sampled by inserting zeros at odd indices and shifting filter coefficients by integer units to the right. This yields the level $j = 2$ MODWT high-pass (H_2) and low-pass (G_2) filters, each containing $2M$ filter coefficients. For example, $H_1 = [h_{1,0}, h_{1,1}, ..., h_{1,(M-1)}]$ would yield $H_2 = [h_{2,0}, h_{2,1}, h_{2,2}, h_{2,3}, h_{2,4}, ..., h_{2,(2M-3)}, h_{2,(2M-2)}, h_{2,(2M-1)}] = [h_{1,0}, 0, h_{1,2}, 0, h_{1,4}, ..., 0, h_{1,(M-2)}, 0]$.

6. The scaling coefficients (V_1) of Step 4 are mirrored $2N$ samples to the left and $2N$ samples to the right (similar to Step 1) resulting in a total of $6N$ samples. The mirrored scaling coefficients are then convolved with the level $j = 2$ MODWT high-pass (H_2) and low-pass (G_2) filters of Step 5 to obtain two convolution vectors, which have $(6N + 2M - 1)$ samples each (similar to Step 2). The level $j = 2$ MODWT wavelet (W_2) and scaling (V_2) coefficients are obtained by selecting samples from indices $2N$ to $(4N - 1)$ from the two convolution vectors (similar to Step 3). Again, the wavelet (W_2) and scaling (V_2) coefficients have $2N$ samples each.

7. The above procedure is repeated for each subsequent level whereby the scaling coefficients V_j of the preceding level j become the input to the next level ($j+1$), resulting in a pyramidal wavelet decomposition scheme.

Fig. 1.   MODWT algorithm.

$L_j = [(2^j - 1)(M - 1) + 1]$ // equivalent filter width, $M \rightarrow$ original filter width

$B_j = (2N - L_j + 1)$ // non boundary coefficients, $N \rightarrow$ samples in input signal

$\lambda_j = 2^{(j-1)}$ // timescale

$$\sigma_j^2(\lambda_j) = \frac{1}{B_j} \sum_{i=L_j-1}^{2N-1} W_j^2[i]$$ // wavelet variance as a function of timescale λ_j

$C_j \equiv 2^j \sigma_j^2(\lambda_j)$ // wavelet spectral density

Fig. 2.   MODWT spectral-density estimation algorithm.

extended before it is convolved with the high-pass (H_j) and low-pass (G_j) wavelet filters. For each decomposition level j (timescale $\lambda_j = 2^{(j-1)}$) of the MODWT (Fig. 1), the spectral density C_j is computed on wavelet coefficients W_j as per the algorithm in Fig. 2. The plot of $\log(C_j)$ versus $\log(\lambda_j)$ is called the wavelet spectral density plot. Fig. 3 demonstrates the computation of the MODWT spectral density metric on an HRV signal. We computed the area under the curve (AUC) of the wavelet spectral density plot to characterize HRV.

Details of other HRV metrics that we assessed can be found in [45] and [46]. In Table I, we present a summary of all variability metrics that were employed for our analysis. A total of eight HRV metrics—wavelet analysis, mean, SD, RMSSD, SampEn, FFT, DFA, and Poincaré plot analysis—were computed. These eight HRV metrics produced a total of 13 HRV parameters (Table I).

Variability was computed on each of the five HRV signals $\{\text{UFIT}_k | k = 1, ..., 5\}$ acquired by the UFIT® BP monitor for each subject. This resulted in five measures of variability for each subject, $\{(\text{HRV}_k | k = 1, ..., 5)_v | v = 1, ..., 13\}$, where v stands for each HRV parameter computed. Thus, we had five sets of 13 HRV parameters for each subject.
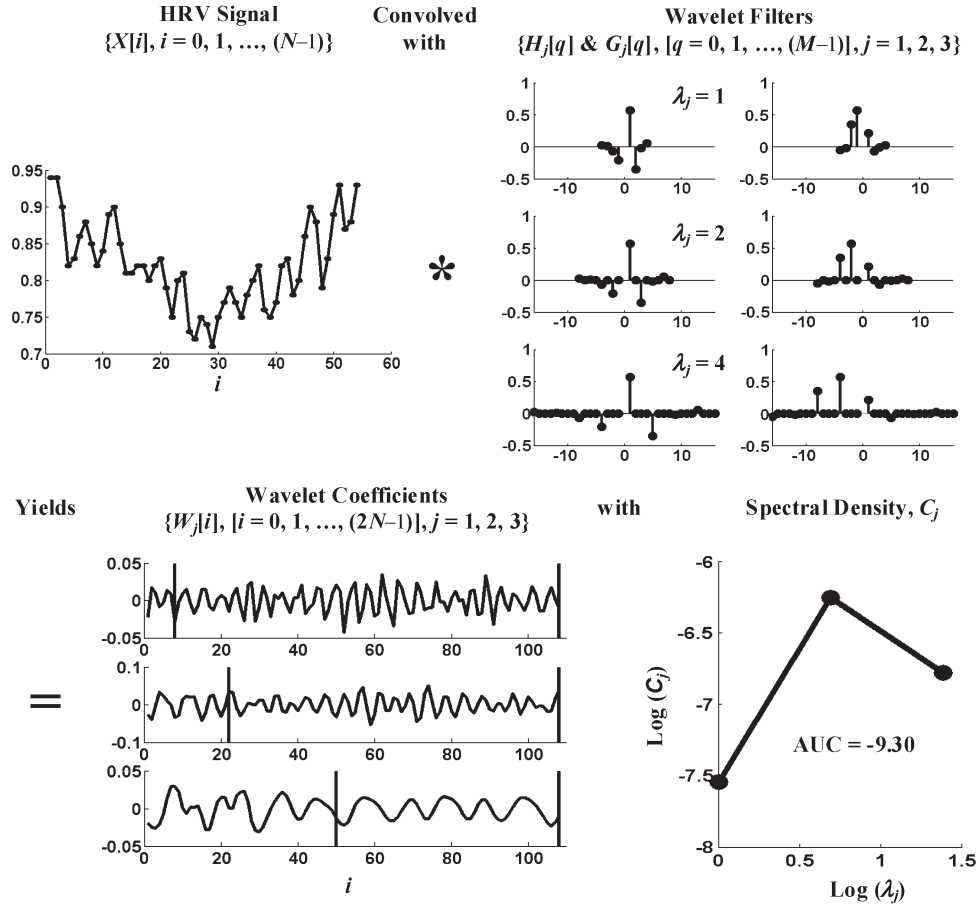
Fig. 3.   Demonstration of the computation of the MODWT spectral-density metric on an HRV signal. See algorithms in Figs. 1 and 2 for more details.

E. Aggregating HRV and BP Data

To aggregate HRV, we computed the average of five HRV values for each subject, $\{[(1/5)\Sigma(\text{HRV}_k)|k = 1, \ldots, 5]_v|v = 1, \ldots, 13\}$, where v stands for each HRV parameter computed. Thus, after the HRV aggregation process, we had one set of 13 HRV parameters for each subject.

The oscillometric BP signals collected for this study are of variable durations. This is because the signals are as long as it took the automated oscillometric BP monitor to complete a measurement. That is, the signal durations vary from recording to recoding and from subject to subject. Therefore, to aggregate signal duration, we computed the average of five signal durations for each subject $\{(1/5)\Sigma(\text{Duration}_k)|k = 1, \ldots, 5\}$. This resulted in one aggregated signal duration for each subject.

To aggregate classic BP measurements, we computed the average of two systolic and two diastolic values recorded by nurses 1 and 2 $\{(\text{SP}_{1,k} + \text{SP}_{2,k})/2, (\text{DP}_{1,k} + \text{DP}_{2,k})/2|k = 1, \ldots, 5\}$. This resulted in five systolic and five diastolic BP values for each subject. We then computed the average of five systolic $\{(1/5)\Sigma[(\text{SP}_{1,k} + \text{SP}_{2,k})/2]|k = 1, \ldots, 5\}$ and five diastolic $\{(1/5)\Sigma[(\text{DP}_{1,k} + \text{DP}_{2,k})/2]|k = 1, \ldots, 5\}$ BP values for each subject. This resulted in one systolic and one diastolic BP value for each subject. Mean arterial pressure [47] was computed as $\text{MAP} = \text{diastolic} + 1/3 * (\text{systolic-diastolic})$, resulting in one MAP value for each subject.

The HRV and BP aggregation process resulted in 13 HRV parameters, 1 signal duration, 1 systolic, 1 diastolic, and 1 MAP value for each subject.

F. Correlating HRV With Age and BP

All 13 HRV parameters and signal duration (a total of 14 parameters) per subject were correlated with the corresponding subject age, systolic BP, diastolic BP, and MAP using a linear regression analysis. We used classic (nurse-recorded) systolic, diastolic, and MAP values for this analysis. The correlation analysis was performed on both genders together ($N_T = 85$) and separately on females ($N_F = 37$) and males ($N_M = 48$). A correlation and p-value was calculated for each least square fit to the linear regression plot at a 95% confidence level.

Correlations of HRV with age and BP are well known and widely reported in the literature. Therefore, the aim of studying correlations of the measured HRV with age and BP was to test the accuracy of our method by comparing our results with the published work.

G. Correlating HRV Metrics

To study the relationship among HRV metrics, Pearson's linear correlation analysis was performed between each pair of HRV metrics for all subjects ($N_T = 85$). To study the dependence of variability on signal duration, we included the signal

TABLE I
SUMMARY OF VARIABILITY METRICS COMPUTED ON THE HRV SIGNALS

Domain	HRV Metric	HRV Parameter	Summary
Time	Mean	Mean	Computed as M = (1/N)$\sum$(PP$_i$), i = 1 to N, where PP$_i$ is ith of N inter-beat intervals. Mean heart rate in beats per minute is given by 60/M since unit of M is seconds.
	Standard Deviation (SD)	SD	Computed as SD = [(1/N)$\sum$(PP$_i$-M)^2]$^{1/2}$, i = 1 to N, where PP$_i$ is ith of N inter-beat intervals and M is their mean. Measures signal variability from its mean value.
	Root Mean Square Successive Difference (RMSSD)	RMSSD	Computed as RMSSD = [{1/(N-1)}$\sum$(PP$_i$-PP$_{i-1}$)^2]$^{1/2}$, i = 2 to N, where PP$_i$ is ith of N inter-beat intervals. Measures variability of successive signal values.
Frequency / Time-Frequency	Fast Fourier Transform (FFT)	LF, HF, LF/HF	Computed by transforming PP interval signal to frequency domain. AUC of bands (HF: 0.18-0.4 Hz, LF: 0.04-0.15 Hz) in power spectrum plot characterizes signal variability.
	Maximal Overlap Discrete Wavelet Transform (MODWT)	AUC	Computed by transforming PP interval signal to time-frequency domain by convolving it with least asymmetric 8-tap (LA8) wavelet filter. AUC of spectral density plot characterizes variability (fluctuations) in time and frequency simultaneously.
Complexity	Sample Entropy (SampEn)	SampEn	Computed as negative logarithm of estimate of conditional probability that PP interval epochs of length m that match pointwise within tolerance r also match at the next point. Characterizes "meaningful structural richness", information, or disorder of signal.
Fractal	Detrended Fluctuation Analysis (DFA)	AUC	Computed as overall root-mean-square fluctuation F(n) of integrated and detrended PP interval signal on multiple timescales n. Linear log-log plot of F(n) versus n indicates fractal scaling and AUC (or intercept) and slope characterizes variability.
Nonlinear	Poincaré Plot Analysis	SD1, SD2, SD2/SD1, Theta	Computed by plotting PP$_i$ on the X axis versus PP$_{i+1}$ on the Y axis, where PP$_i$ is ith of N inter-beat intervals. Minor axis (SD1), major axis (SD2), and orientation (theta) of the resulting elliptical cloud characterizes variability.

duration in this analysis. We produced a correlation matrix with $C(n, 2) = n!/(2!(n-2)!)$ elements, where n is the number of HRV parameters measured, including the signal duration. Thus, for n = 14 (13 HRV parameters + 1 signal duration), we produced a correlation matrix with 91 elements (or correlations).

H. Multiple-Regression Analysis

We performed multiple-linear-regression analysis of various combinations of HRV metrics with age, classic systolic, diastolic, and MAP BP values. The multiple regression analysis was performed by employing a *training–testing* paradigm, whereby a regression model was built on the *training* data, and this *training* model was used to predict the age and BP values in the *testing* data. We trained on 75% of the data (randomly chosen) and tested on the remaining 25% to ensure that we do not overfit the data. The performance of the multiple regression model was assessed based on the computation of Pearson's linear correlation between the actual and predicted age and BP values and mean absolute error (MAE), {MAE = $(1/n)\Sigma(|f_i - y_i|)|i = 1, \ldots, n$}, where f_i is the prediction, y_i is the true value, and n is the number of subjects in the *testing* set.

The multiple-linear-regression analysis was performed on both genders together ($N_T = 85$) and separately on females ($N_F = 37$) and males ($N_M = 48$). For each of the three populations ($N_T = 85, N_F = 37, N_M = 48$), a total of ten *training–testing* datasets were formed as described in the pre-

vious paragraph, and a regression analysis was performed on each of these datasets. The overall age and BP prediction performance of the regression model was evaluated by averaging the correlation and MAE values for the ten datasets.

The aim of the multiple-regression analysis was to evaluate whether the correlations between the predicted and actual age and the predicted and actual BP could be improved compared to single-regression modeling. Such an improvement would point towards multiple HRV metrics offering a more comprehensive characterization of variability than that offered by single metrics.

III. RESULTS

In Fig. 4, we present the results of the correlations of different HRV metrics with age and BP. Correlations are studied for both genders together ($N_T = 85$) and separately for females ($N_F = 37$) and males ($N_M = 48$). A black bar represents a significant correlation ($p < 0.05$), whereas a gray bar represents a correlation that is not significant ($p \geq 0.05$). A positive or negative sign beside each HRV metric indicates whether the correlation is direct or inverse. The MODWT HRV metric achieves the best overall performance. It shows the maximum number of the highest (and most significant) inverse correlations with age and BP. The RMSSD metric is the next best in performance. It achieves the highest (and most significant) negative correlations with diastolic BP for all (both genders together),
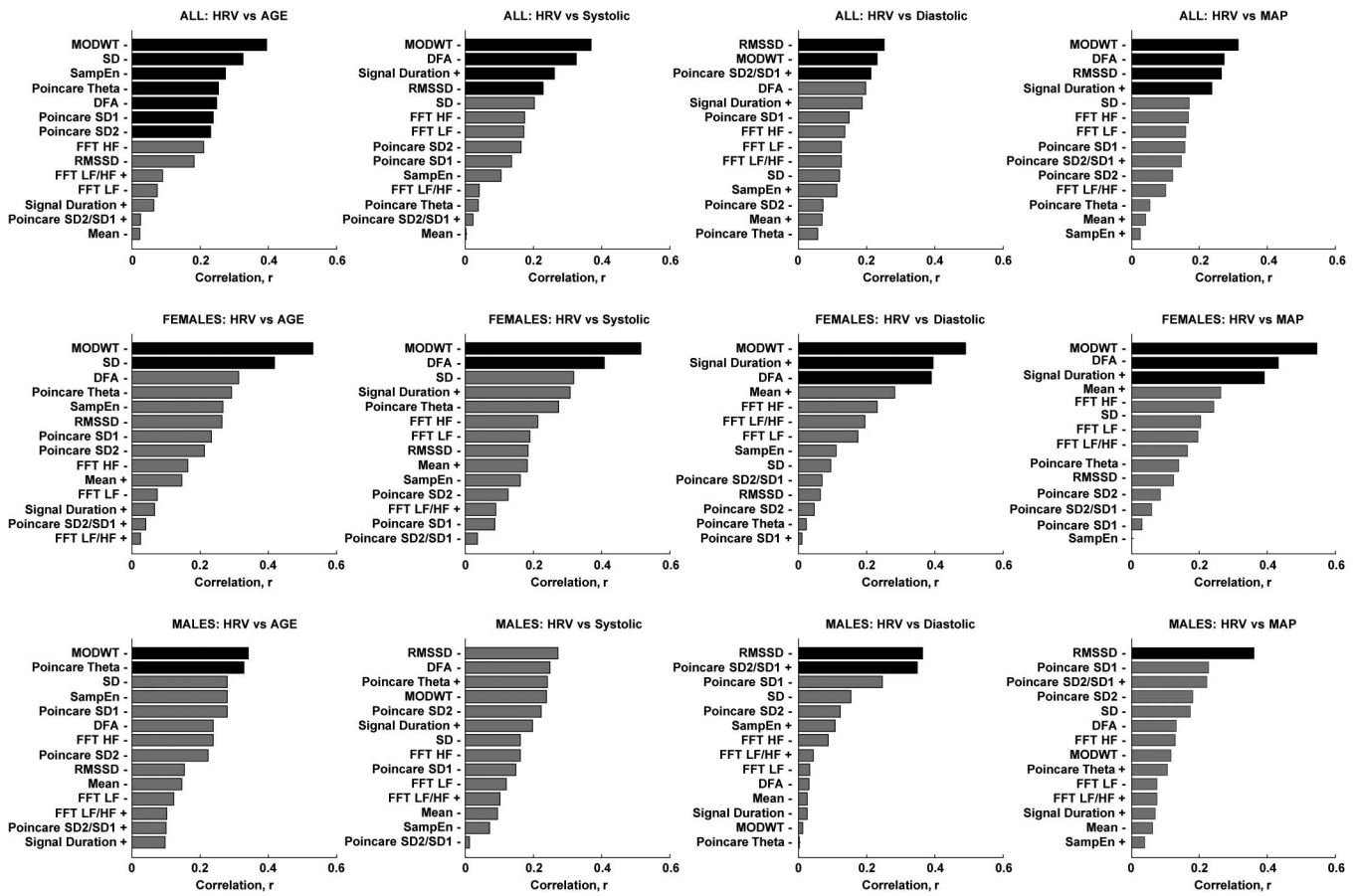
Fig. 4. Correlations between HRV and age and between HRV and BP. A black bar represents a significant correlation ($p < 0.05$), whereas a gray bar represents a correlation that is not significant ($p \geq 0.05$). A $\pm$ sign beside each HRV parameter indicates whether the correlation is direct or inverse.

TABLE II
COMPARISON OF THE HRV−AGE CORRELATIONS ACHIEVED BY THE MODWT METRIC WITH OTHER PUBLISHED WORK

HRV and Age Correlation Comparison							
Author	Signal Analyzed	Signal Duration (s)	Sample Size (N)	Gender	HRV Metric	HRV-Age Correlation	P-value
Choi et al. [15]	ECG	180	135	M + F	FFT LF	-31%	p<0.01
					FFT HF	-42%	p<0.01
					FFT LF/HF	15%	p>0.09
Bonnemeier et al. [16]	ECG	86400	166	M + F	RMSSD	-62%	p<0.001
			81	F	RMSSD	-56%	p<0.001
			85	M	RMSSD	-65%	p<0.001
Kim et al. [17]	ECG	300	41	M + F	SD	-42%	p<0.01
					FFT LF	-54%	p<0.01
					FFT HF	-46%	p<0.01
Ahmad et al.	Oscillometric Waveform	31-95	85	M + F	MODWT	-40%	p<0.001
			37	F	MODWT	-53%	p<0.001
			48	M	MODWT	-34%	p<0.05

diastolic BP for males, and MAP for males. None of the HRV metrics achieve a significant correlation with systolic BP for males.

In Table II, we present a comparison of the HRV−age correlations achieved by the MODWT metric with other published work. The values of correlations with age that the MODWT metric achieves are in range with values of correlations reported by other researchers on significantly longer and constant-duration ECG signals.

A comparison of the correlations between HRV and BP achieved by the MODWT metric with other published work is presented in Table III. Again, the correlation values achieved by

TABLE III
COMPARISON OF THE HRV–BP CORRELATIONS ACHIEVED BY THE MODWT METRIC WITH OTHER PUBLISHED WORK

HRV and BP Correlation Comparison									
Author	Signal Analyzed	Signal Duration (s)	BP Monitor	Sample Size (N)	Gender	HRV Metric	BP Measurement	HRV-BP Correlation	P-value
Virtanen et al. [7]	ECG	300	Classic	296	M + F	FFT LF	MAP	-13%	p<0.05
						FFT HF	MAP	-16%	p<0.01
						SD	MAP	-13%	p<0.05
						RMSSD	MAP	-14%	p<0.05
Mussalo et al. [8]	ECG	250	Classic	34	M + F	RMSSD	Systolic	40%	p<0.01
						FFT LF	Diastolic	-17%	p>0.01
Huikuri et al. [9]	ECG	2700	Automatic Oscillometric	168	M	FFT LF	Systolic	-20%	p<0.001
						FFT HF	Systolic	-20%	p<0.001
Ahmad et al.	Oscillometric Waveform	31-95	Classic	85	M + F	MODWT	Systolic	-37%	p<0.001
						MODWT	Diastolic	-23%	p<0.05
						MODWT	MAP	-32%	p<0.005
				37	F	MODWT	Systolic	-52%	p<0.005
						MODWT	Diastolic	-49%	p<0.005
						MODWT	MAP	-55%	p<0.005

TABLE IV
COMPARISON BETWEEN THE MODWT AND THE DWT SPECTRAL-DENSITY HRV METRICS THAT EMPLOY DIFFERENT WAVELET FILTERS

Comparison Between MODWT and DWT Employing Different Filters						
Filter	Sample Size (N)	Gender	MODWT		DWT	
			HRV-Age Correlation	P-Value	HRV-Age Correlation	P-Value
Haar	85	M + F	-37%	0.0004	-32%	0.003
D4	85	M + F	-38%	0.0003	-32%	0.003
C6	85	M + F	-39%	0.0003	-31%	0.003
LA8	85	M + F	-40%	0.0002	-31%	0.003
		Mean	-38%	0.0003	-32%	0.003
		SD	0.8%	9.4E-05	0.2%	1.7E-04

the MODWT HRV metric are well in range or even higher than the correlation values reported by other researchers on much longer and constant-duration ECG signals.

In Table IV, we present a comparison between the MODWT and the classical discrete wavelet transform (DWT) spectral-density HRV metrics employing different wavelet filters. To this end, we study the correlations between HRV and age for both genders ($N_T = 85$). Our results indicate that the choice of the wavelet filter does not significantly affect the correlation between HRV and age for either the MODWT (SD of $r = 0.8\%$) or the DWT (SD of $r = 0.2\%$) metric. However, for different filters, the MODWT metric consistently achieves a higher and more significant correlation with age (Mean $r = -38\%$, Mean $p = 0.0003$) compared to the DWT metric (Mean $r = -32\%$, Mean $p = 0.003$). In addition, the highest and most significant correlation ($r = -40\%$, $p = 0.0002$) is achieved by the MODWT metric that employs the LA8 filter.

For estimating the wavelet spectral density, Percival and Walden prefer MODWT over DWT due to the poor statistical properties of DWT [28]. For DWT, these poor statistical properties arise due to the downsampling of the signal at each decom-

position level and the lack of translational invariance. MODWT avoids these disadvantages to provide a statistically superior estimation of the wavelet spectral density. Moreover, the LA8 wavelet filter is designed to be an approximate zero-phase filter with ideal bandpass properties, making it an efficient estimator of the wavelet spectral density [28], [44].

Therefore, our empirical findings and an analysis of relevant literature justify the use of the MODWT HRV metric that employs the LA8 wavelet filter to characterize HRV from short-duration oscillometric BP signals.

The correlation matrix in Table V shows Pearson's correlations between all HRV parameters for all subjects ($N_T = 85$). The highest correlation ($r = 93\%$) is achieved between the MODWT and DFA metrics of HRV. Other HRV metrics that show a significantly high correlation ($r \geq 90\%$) are SD and RMSSD ($r = 91\%$), SD and Poincaré SD1 ($r = 91\%$), SD and Poincaré SD2 ($r = 91\%$), and Poincaré SD1 and RMSSD ($r = 90\%$).

Fig. 5 shows snapshots of predicting age and BP using multiple-linear-regression modeling. The left-hand plot shows results of using one of the ten datasets (dataset #3) for

TABLE V
CORRELATION MATRIX THAT SHOWS PEARSON'S CORRELATIONS BETWEEN ALL HRV PARAMETERS FOR ALL SUBJECTS ($N_T = 85$).
CORRELATIONS GREATER THAN OR EQUAL TO 90% APPEAR IN BOLD FONT AND ARE UNDERLINED

| $N_T = 85$	MODWT	DFA	RMSSD	Mean	Poincaré SD1	Poincaré SD2	Poincaré SD2/SD1	Poincaré Theta	SampEn	SD	FFT HF	FFT LF	FFT LF/HF
DFA	**93%**												
RMSSD	57%	55%											
Mean	-58%	-65%	-38%										
Poincaré SD1	58%	57%	**90%**	-32%									
Poincaré SD2	63%	61%	83%	-45%	80%								
Poincaré SD2/SD1	-15%	-20%	-40%	8%	-50%	2%							
Poincaré Theta	17%	15%	13%	2%	31%	-15%	-74%						
SampEn	17%	15%	0%	-15%	2%	-1%	-12%	29%					
SD	70%	65%	**91%**	-43%	**91%**	**91%**	-23%	14%	6%				
FFT HF	72%	82%	52%	-69%	49%	56%	-15%	6%	-1%	58%			
FFT LF	54%	67%	13%	-49%	10%	17%	-4%	2%	-7%	18%	80%		
FFT LF/HF	31%	38%	-14%	-24%	-15%	-14%	0%	5%	-12%	-10%	41%	81%	
Signal Duration	-75%	-89%	-28%	60%	-29%	-34%	15%	-7%	-3%	-35%	-78%	-73%	-50%
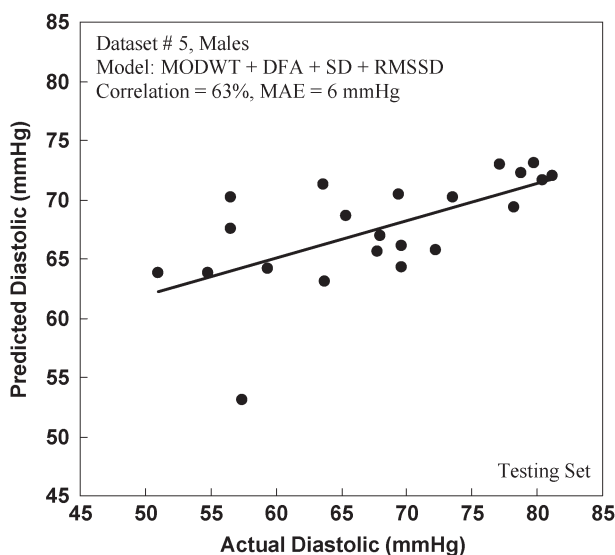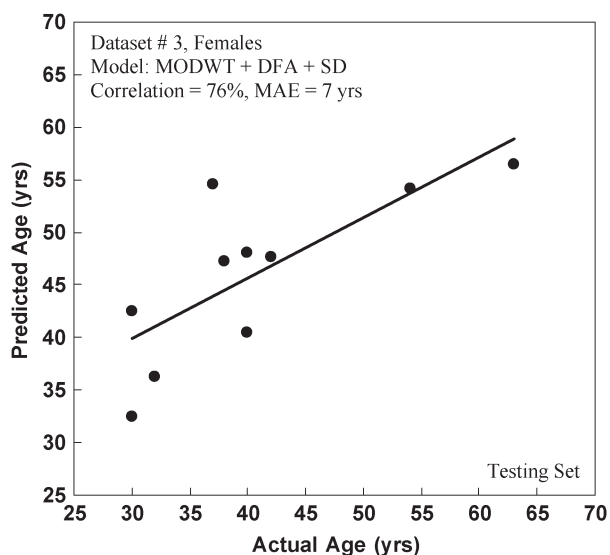
Fig. 5. Snapshots of predicting age and BP using multiple-regression modeling.

predicting the female age by employing MODWT + DFA + SD in the multiple-regression model. A correlation of 76% is achieved between the actual and predicted female ages in the *testing* set. The right-hand plot shows results of dataset #5 for predicting the male diastolic BP by employing MODWT + DFA + SD + RMSSD in the multiple-regression model. A correlation of 63% is achieved between the actual and predicted male diastolic BP in the *testing* set.

A summary of multiple-linear-regression analysis for predicting age and BP is presented in Table VI. Models based on combinations of the MODWT, DFA, SD, and RMSSD measures of HRV are tested for predicting age and BP. Males and females are studied together ($N_T = 85$) and separately ($N_F = 37, N_M = 48$), and average results (correlation and MAE) for all the ten datasets are reported. For each prediction of age and BP, different combinations of the MODWT metric with

TABLE VI
SUMMARY OF MULTIPLE-REGRESSION ANALYSIS FOR PREDICTING AGE AND BP. COMBINING OTHER METRICS
WITH MODWT IMPROVES PREDICTIONS (BOLD UNDERLINED NUMBERS)

| | | | | | | Multiple Regression Analysis | | | | | | | |
| Gender | Model | Number of Datasets | Sample Size (N) | Trained On | Tested On | Predicted Age vs Actual Age | | Predicted Systolic vs Actual Systolic | | Predicted Diastolic vs Actual Diastolic | | Predicted MAP vs Actual MAP | |
						Correlation	Mean Absolute Error (yrs)	Correlation	Mean Absolute Error (mmHg)	Correlation	Mean Absolute Error (mmHg)	Correlation	Mean Absolute Error (mmHg)
Males + Females	MODWT	10	85	63	22	34%	11.62	38%	10.29	30%	7.78	36%	8.08
	MODWT + DFA	10	85	63	22	**55%**	**10.02**	29%	10.89	20%	6.95	27%	7.51
	MODWT + DFA + SD	10	85	63	22	39%	10.99	**38%**	**9.91**	16%	7.47	30%	7.51
	MODWT + DFA + SD + RMSSD	10	85	63	22	38%	10.54	27%	11.20	**42%**	**7.48**	**39%**	**8.10**
Females	MODWT	10	37	27	10	42%	10.86	36%	11.79	43%	8.13	44%	8.72
	MODWT + DFA	10	37	27	10	58%	9.15	**46%**	**11.64**	44%	8.20	52%	8.46
	MODWT + DFA + SD	10	37	27	10	**60%**	**9.57**	29%	11.47	40%	7.42	40%	7.80
	MODWT + DFA + SD + RMSSD	10	37	27	10	52%	9.83	43%	11.27	**55%**	**6.66**	**56%**	**7.22**
Males	MODWT	10	48	36	12	40%	10.20	22%	9.27	-8%	6.44	14%	6.76
	MODWT + DFA	10	48	36	12	**47%**	**11.37**	18%	10.39	-17%	7.66	0%	7.98
	MODWT + DFA + SD	10	48	36	12	31%	10.63	17%	10.23	6%	7.34	0%	7.87
	MODWT + DFA + SD + RMSSD	10	48	36	12	33%	11.19	**23%**	**10.99**	**45%**	**6.21**	**32%**	**7.17**

DFA, SD, and RMSSD improve predictions compared to the predictions achieved by the MODWT metric alone. For example, for predicting the female age, the MODWT model, on its own, achieves a correlation of 42% and an MAE of 10.86 years. When a model that employs MODWT + DFA + SD is used to predict the female age, a correlation of 60% and an MAE of 9.57 years is achieved. The best prediction (highest correlation and lowest MAE) for each predicted parameter appears in bold underlined font in Table VI.

We have employed a combination of different HRV metrics inside a simple multiple-linear- regression model for predicting age and BP to evaluate whether combining HRV metrics offers improved predictions and, hence, better characterization of variability (Table VI) compared to single metrics. Other researchers have employed principal component analysis (PCA) and neural networks (NN) to predict age. Colosimo *et al.* employed PCA to predict age in healthy subjects ($N = 141$) by analyzing 512-s-long segments of ECG signals [18]. They report a correlation of 71% between the actual and predicted ages. However, it seems that they trained and tested on the same data ($N = 141$); thus, overfitting cannot be ruled out.

In Table VII, we report the results of our multiple-linear-regression analysis in light of the results reported by Corino *et al.* [19], who employed a combination of PCA and NN to predict age. Corino *et al.* report higher correlations than those achieved by our multiple-linear-regression models. However, they have used 24-h-long ECG signals and employed 16 principal components (PCS; 100% kept variance), whereas we have used short (31–95 s) oscillometric signals and employed two to four HRV regressors. Moreover, Corino *et al.* report an average of three sets of training–testing data, where the system was trained and validated on 89% of the data and tested on the remaining 11%. In comparison, we report an average of ten datasets, where the system was trained on 75% of the data and tested on the remaining 25% of the data.

In this study, we measured HRV from short-duration oscillometric BP signals for 85 subjects. For these subjects, we did not record simultaneous ECG signals for cross validating the accuracy of the proposed HRV measurement method. The correlations of the measured HRV with age and BP conformed to earlier published work (of HRV analysis on much longer ECG signals), thus validating the accuracy of our method.

TABLE VII
COMPARISON OF ACTUAL VERSUS PREDICTED AGE CORRELATIONS ACHIEVED BY OUR MULTIPLE-LINEAR-REGRESSION
ANALYSIS WITH OTHER PUBLISHED WORK.

| Actual and Predicted Age Correlation Comparison											
Author	Signal Analyzed	Signal Duration (s)	Sample Size (N)	Gender	Training Set (% of N)	Validation Set (% of N)	Testing Set (% of N)	Number of Datasets	Model	Regressors	Average Testing Set Correlation (Predicted vs Actual Age)
Corino et al. [19]	ECG	81000	131	M + F	67%	22%	11%	3	PCA-FFNN	16 HRV PCs	88%
			131	M + F	67%	22%	11%	3	PCA-RBFNN	16 HRV PCs	70%
Ahmad et al.	Oscillometric Waveform	31-95	85	M + F	75%	0%	25%	10	Multiple Regression	MODWT + DFA	55%
			37	F	75%	0%	25%	10	Multiple Regression	MODWT + DFA + SD	60%
			48	M	75%	0%	25%	10	Multiple Regression	MODWT + DFA	47%
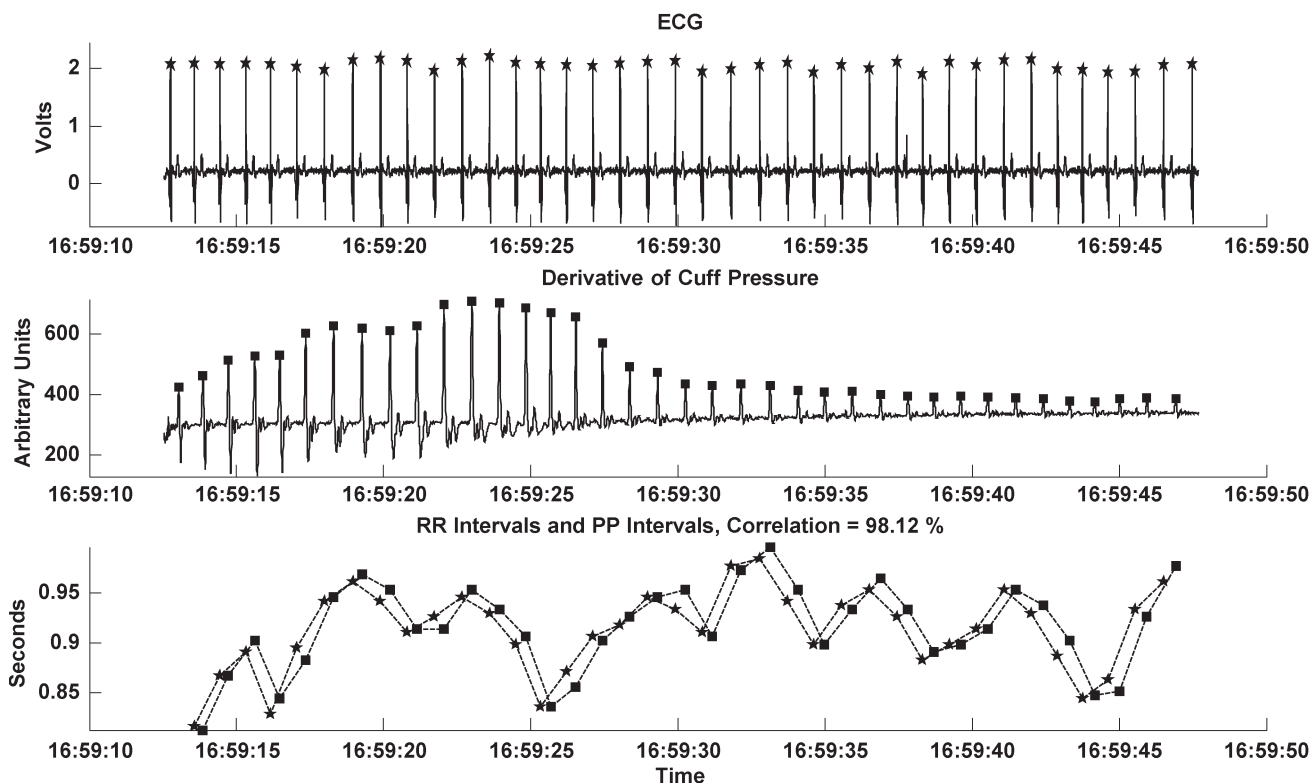
Fig. 6. Comparison of the pulse wave signal (second panel) acquired by the UFIT® automated oscillometric wrist BP monitor with a simultaneous ECG signal (first panel) acquired by the BioHarness™ chest belt telemetry system for Subject 1. A similarity in patterns and a correlation of 98% is observed between ECG-based RR intervals and pulse-wave-based PP intervals (third panel).

However, as an additional step in the validation of the accuracy of our proposed HRV measurement method, we analyzed the oscillometric BP signals acquired by the UFIT® device, along with simultaneously recorded ECG signals for four healthy subjects (two males and two females). ECG

signals were collected using a chest-belt telemetry system (BioHarness™, Zephyr Technology Ltd., Auckland, New Zealand) at a sampling rate of 250 Hz.

Fig. 6 shows the oscillometric pulse wave signal acquired by the UFIT® device (second panel), along with a simultaneous

TABLE VIII
SUMMARY OF THE ANALYSIS ON UFIT® PP INTERVALS AND THE SIMULTANEOUS BIOHARNESS™ RR INTERVALS FOR FOUR HEALTHY SUBJECTS.
CORRELATIONS ARE STUDIED BETWEEN RR AND PP INTERVAL TIME SERIES. IN ADDITION, FIVE HRV PARAMETERS
ARE ASSESSED FOR THE RR AND PP INTERVAL TIME SERIES

Comparison Between Pulse Wave and ECG HRV						Heart Rate Variability (HRV)				
Subject #	Gender	Age (yrs)	Signal Duration (s)	RR-PP Correlation	Measure	Mean HR (BPM)	SD	RMSSD	FFT LF/HF	MODWT AUC
1	M	23	35	98%	ECG Based HRV	66	0.041	0.0373	16.03	-9.11
					Pulse Wave Based HRV	66	0.044	0.0401	16.16	-8.92
2	M	36	36	96%	ECG Based HRV	69	0.051	0.0372	12.80	-8.97
					Pulse Wave Based HRV	69	0.053	0.0416	12.28	-8.77
3	F	24	35	99%	ECG Based HRV	74	0.054	0.0470	12.86	-8.26
					Pulse Wave Based HRV	74	0.060	0.0521	12.64	-8.02
4	F	21	37	98%	ECG Based HRV	61	0.066	0.0555	13.65	-7.53
					Pulse Wave Based HRV	60	0.064	0.0576	13.81	-7.57

ECG signal acquired by the BioHarness™ device (first panel) for Subject # 1. The pulse wave signal acquired by the UFIT® device appears clean and resembles a typical oscillometric BP signal. The third panel in Fig. 6 shows the corresponding RR and PP intervals. We note that the patterns of the RR and PP interval time series are similar, and a correlation of 98% is observed between the two.

In Table VIII, we present a summary of the analysis on the UFIT®-derived PP intervals and the simultaneous BioHarness™-derived RR intervals for all the four subjects. For each subject, correlations are studied between RR and PP interval time series. In addition, five HRV parameters are assessed for the RR and PP interval time series. An RR–PP correlation in the range of 96%–99% is observed for all four subjects. Moreover, the values of the ECG-based and pulse-wave-based HRV parameters are similar for all four subjects.

Therefore, results of the analysis of oscillometric BP signals acquired by the UFIT® device, along with the simultaneously recorded ECG signals, for four healthy subjects further validate the accuracy of our proposed HRV analysis method.

IV. CONCLUSION

This is the first study in which an automated oscillometric BP monitor has been utilized for measuring HRV. We have employed the MODWT-based spectral density estimation method for characterizing HRV from short pulse wave signals of variable durations (range: 31–95 s; median: 55 s), acquired by an automated oscillometric BP monitor during routine measurements. To assess the MODWT HRV metric, we compared its performance with a number of alternative HRV metrics and earlier published work. The MODWT HRV metric shows an overall higher accuracy in characterizing HRV by achieving the

maximum number of high (and most significant) correlations with age and BP compared to other techniques (Fig. 4). In addition, our results show that the performance of the MODWT HRV metric in analyzing short-duration oscillometric BP signals is at par with the techniques used by other researchers to characterize variability from significantly longer duration ECG signals. This result is validated by the fact that values of correlations (with age and BP) achieved by the MODWT HRV metric are in good agreement with the correlation values reported by other researchers (Tables II and III).

The wavelet method that we employed (MODWT) and those employed by other researchers, e.g., Lin *et al.*, Thurner *et al.*, Ivanov *et al.*, and Verlinde *et al.*, for transforming HRV signals into the time–frequency domain are principally the same, with only slight differences in how variability is computed. Given the short durations of our HRV signals, we found that the MODWT spectral density estimation method that employs the LA8 wavelet filter is empirically the best suited and the most effective for characterizing HRV (Table IV).

After the MODWT metric, the RMSSD metric was the next best in performance, followed by the DFA and SD metrics (Fig. 4). However, these techniques did not show the same robustness and consistency in characterizing HRV as shown by the MODWT metric. That is, they did not achieve significant and steady correlations with age and BP similar to MODWT. We attribute the success of the MODWT metric to the fact that wavelet analysis is a recursive filtering technique that simultaneously characterizes a signal in both time and frequency domains. This renders the wavelet analysis as a robust tool for assessing signals that are noisy, nonstationary, and nonperiodic. The fact that the analyzed signals were of extremely short durations seems to have left other techniques more sensitive to even small amounts of noise, nonstationarity, and nonperiodicity that

may have been present in these signals. On the other hand, the MODWT metric that employs a filtered time–frequency characterization of variability coped better with these signals.

The HRV measured from oscillometric BP signals showed different correlations with different physiological parameters, i.e., age, systolic BP, diastolic BP, and MAP (Fig. 4). These results are in line with the results obtained by other researchers who also found different correlations between HRV and different physiological parameters (Tables II and III). Although not the focus of this study, an in depth investigation into the physiology of altered HRV may throw more light on the explanations and interpretations of different correlations between HRV and different physiological parameters.

We have observed that oscillometric pulse wave signal duration was correlated with BP. For example, for females, signal duration showed a correlation of $+40\%(p < 0.05)$ with diastolic BP (Fig. 4). That is, a higher BP resulted in a longer oscillometric pulse wave signal. This observation can be explained by the fact that the UFIT $\circledR$ automated oscillometric BP monitor establishes a rough estimate of a subject's BP before initiating a BP measurement or the process of inflation and deflation of the cuff. For example, for a subject whose BP is estimated to be high by the monitor, it inflates the cuff to a desired higher pressure. Hence, the resulting oscillometric signal duration is longer, because it takes the monitor longer to deflate the cuff back to zero pressure from this higher starting pressure. Therefore, if the monitor makes correct initial assessments of the actual BP values, it is expected that durations of acquired oscillometric signals would be proportional to actual BP values.

The analysis of correlations among HRV metrics produced interesting results. For example, the highest correlation (93%) was achieved between the MODWT and DFA metrics of HRV (Table V). This is understandable since the DFA, like the MODWT, is a multiscaling technique whereby fluctuations are studied by detrending the signal at different timescales or bin sizes. However, despite such a high correlation with MODWT, DFA could not perform as well as MODWT for characterizing HRV. We observe that, based on the DFA algorithm, short signal durations would only allow for a small number of bins to be made. Therefore, we believe that the process of detrending and measuring fluctuations in a limited number of bins with only few samples did not result in an accurate-enough characterization of variability by the DFA metric.

Multiple-linear-regression analysis for predicting age and BP showed that combining other HRV metrics with the MODWT metric consistently resulted in a better performance than that achieved by the MODWT metric alone (Table VI). We have experimented with various combinations of the HRV metrics for predicting age and BP. We empirically found that combining the MODWT metric with the SD, RMSSD, and DFA metrics, in particular, yields the best performance.

The correlations between the actual and predicted ages achieved by our simple multiple-regression models were lower than those reported by other researchers who employed PCA and NN (Table VII). However, our goal was not to fit the data or to provide precise predictions of age or BP by employing multiple regressions. It was, rather, to evaluate whether the use of multiple HRV metrics offers better characterization of variability. In this light, the results of our multiple-linear-regression analysis are noteworthy. An improvement in predicting age and BP by combining other HRV metrics with the MODWT metric suggests that multiple measures provide a more comprehensive characterization of HRV compared to single measures.

As an additional step in the validation of the accuracy of our HRV measurement method, we have analyzed oscillometric BP signals acquired by the UFIT $\circledR$ BP monitor, along with simultaneously recorded ECG signals, for four healthy subjects. A correlation in the range of 96%–99% between RR–PP time series and the closeness between ECG and pulse wave HRV parameters confirmed that the fidelity of HRV that our method offers is equivalent to that offered by the classical ECG-based method (Fig. 6 and Table VIII).

Based on our results and the aforementioned discussion, we conclude that it is possible to accurately measure HRV by utilizing an automated oscillometric BP monitor. Moreover, multiple measures of HRV provide a better and more comprehensive characterization of variability than single measures. Therefore, incorporating a multiparameter HRV module inside a conventional automated oscillometric BP monitor promises to provide quick and accurate tracking of variability.

The proposed method of measuring HRV utilizing an automated wrist BP monitor offers certain advantages over the classical ECG-based method. It takes an oscillometric BP monitor only about 30–90 s to acquire a pulse wave signal. Thus, our method can more conveniently provide an accurate assessment of HRV within this timeframe compared to ECG-based or other HRV estimation methods, which require much longer monitoring (≥ 180 s). Our method is less intrusive than the ECG-based method, because we collect oscillometric signals from the wrist as opposed to ECG data acquisition, which requires chest electrodes or a chest belt. Finally, our method is more economical, because commercially available wrist BP monitors are cheaper than commercially available ECG monitors.

The main challenge that we have faced in this study was due to the presence of about 3% noise in our PP interval time series (HRV signals). Because signal durations were extremely short, one or two peaks falsely identified or missed by the peak detection algorithm affected the variability analysis to some extent. We had to manually correct peaks that were falsely identified or missed by the peak detection algorithm before we carried out the variability analysis. We are currently working on fine-tuning our cleaning and peak detection algorithms in an effort to minimize errors and the need for manual peak correction.

Future work would involve exploring the PCA for predicting age and BP. Given that the MODWT HRV metric has shown significant correlations with age and BP and that combining other HRV metrics with the MODWT metric that employs simple multiple linear regressions has improved prediction of these parameters, PCA appears to be a promising alternative for further improving predictions. In particular, an accurate estimation of BP based on multiparameter HRV and PCA would be a pertinent and important contribution toward the analysis of pulse wave signals produced by an automated oscillometric BP monitor during routine measurements.

Numerous new avenues could open with the accurate assessment of HRV from short-duration oscillometric BP signals.

This method could be particularly useful in the assessment of short-term changes in variability following certain physiologic perturbations. For example, our method could be used to characterize variability, following the Valsalva or Mueller maneuvers, which are imposed physiologic perturbations for assessing cardiac function. The assessment of variability following such maneuvers would add a new dimension to the analysis of cardiac function. Our method can also be used to assess short-term variability following sleep apnea, which is a natural physiologic perturbation. It is well known that there are transient changes in HRV following sleep apnea. Our method could be used to effectively study these changes.

Another application of our method could be for detecting cardiac arrhythmias. Because HRV is known to exhibit characteristic signatures during arrhythmias, our method could be used to detect arrhythmias from short-duration oscillometric BP signals. This functionality would be of particular importance in a BP monitor, whereby arrhythmias tend to obfuscate accurate measurement of systolic and diastolic pressure.

ACKNOWLEDGMENT

REFERENCES

[1] P. K. Stein and R. E. Kleiger, "Insights from the study of heart rate variability," *Annu. Rev. Med.*, vol. 50, pp. 249–261, 1999.
[2] R. E. Kleiger, P. K. Stein, M. S. Bosner, and J. N. Rottman, "Time-domain measurements of heart rate variability," *Cardiol. Clin.*, vol. 10, no. 3, pp. 487–498, Aug. 1992.
[3] K. C. Bilchick and R. D. Berger, "Heart rate variability: Frequency-domain measures of HRV," *J. Cardiovasc. Electrophysiol.*, vol. 17, no. 6, pp. 691–694, 2006.
[4] D. E. Lake, J. S. Richman, M. P Griffin, and J. R. Moorman, "Sample entropy analysis of neonatal heart rate variability," *Amer. J. Physiol. Regul. Integr. Comp. Physiol.*, vol. 283, no. 3, pp. 789–797, Sep. 2002.
[5] C.-K. Peng, S. Havlin, H. E. Stanley, and A. L. Goldberger, "Quantification of scaling exponents and crossover phenomena in nonstationary heartbeat time series," *Chaos*, vol. 5, no. 1, pp. 82–87, Mar. 1995.
[6] L. Mourot, M. Bouhaddi, S. Perrey, J. D. Rouillon, and J. Regnard, "Quantitative Poincaré plot analysis of heart rate variability: Effect of endurance training," *Eur. J. Appl. Physiol.*, vol. 91, no. 1, pp. 79–87, Jan. 2004.
[7] R. Virtanen, A. Jula, T. Kuusela, H. Helenius, and L. M. Voipio-Pulkki, "Reduced heart rate variability in hypertension: Associations with lifestyle factors and plasma renin activity," *J. Hum. Hypertens.*, vol. 17, no. 3, pp. 171–179, Mar. 2003.
[8] H. Mussalo, E. Vanninen, R. Ikaheimo, T. Laitinen, M. Laakso, E. Länsimies, and J. Hartikainen, "Heart rate variability and its determinants in patients with severe or mild essential hypertension," *Clin. Physiol.*, vol. 21, no. 5, pp. 594–604, Sep. 2001.
[9] H. V. Huikuri, A. Ylitalo, S. M. Pikkujämsä *et al.*, "Heart rate variability in systemic hypertension," *Amer. J. Cardiol.*, vol. 77, no. 12, pp. 1073–1077, May 1996.
[10] D. Bonaduce, M. Petretta, F. Marciano, M. L. Vicario, C. Apicella, M. A. Rao, E. Nicolai, and M. Volpe, "Independent and incremental prognostic value of heart rate variability in patients with chronic heart failure," *Amer. Heart J.*, vol. 138, no. 2, pp. 273–284, Aug. 1999.
[11] S. Guzzetti, S. Mezzetti, R. Magatelli, A. Porta, G. De Angelis, G. Rovelli, and A. Malliani, "Linear and nonlinear 24-h heart rate variability in chronic heart failure," *Auton. Neurosci.*, vol. 86, no. 1/2, pp. 114–119, Dec. 2000.
[12] M. Piepoli, C. S. Garrard, D. A. Kontoyannis, and L. Bernardi, "Autonomic control of the heart and peripheral vessels in human septic shock," *Intensive Care Med.*, vol. 21, no. 2, pp. 112–119, Feb. 1995.
[13] J. Pontet, P. Contreras, A. Curbelo, J. Medina, S. Noveri, S. Bentancourt, and E. R. Migliaro, "Heart rate variability as early marker of multiple-organ-dysfunction syndrome in septic patients," *J. Crit. Care*, vol. 18, no. 3, pp. 156–163, Sep. 2003.
[14] D. Gallagher, T. Terenzi, and R. Meersman, "Heart rate variability in smokers, sedentary, and aerobically fit individuals," *Clin. Auton. Res.*, vol. 2, no. 6, pp. 383–387, Dec. 1992.
[15] J. Choi, S. Hong, R. Nelesen, W. A. Bardwell, L. Natarajan, C. Schubert, and J. E. Dimsdale, "Age and ethnicity differences in short-term heart rate variability," *Psychosom. Med.*, vol. 68, no. 3, pp. 421–426, May/Jun. 2006.
[16] H. Bonnemeier, U. K. H. Wiegand, A. Brandes, N. Kluge, H. A. Katus, G. Richardt, J. Potratz, T. Kara, J. Nykodym, and V. K. Somers, "Circadian profile of cardiac autonomic nervous modulation in healthy subjects: Differing effects of aging and gender on heart rate variability," *J. Cardiovasc. Electrophysiol.*, vol. 14, no. 8, pp. 791–799, 2003.
[17] J. A. Kim, Y. Park, K. Cho *et al.*, "Heart rate variability and obesity indices: Emphasis on the response to noise and standing," *J. Amer. Board Fam. Pract.*, vol. 8, no. 2, pp. 97–103, Mar./Apr. 2005.
[18] A. Colosimo, A. Giuliani, A. M. Mancini, G. Piccirillo, and V. Marigliano, "Estimating a cardiac age by means of heart rate variability," *Amer. J. Physiol. Heart Circ. Physiol.*, vol. 273, no. 4, pp. 1841–1847, Oct. 1997.
[19] V. D. A. Corino, M. Matteucci, L. Cravello, E. Ferrari, A. A. Ferrari, and L. T. Mainardi, "Long-term heart rate variability as a predictor of patient age," *Comput. Methods Programs Biomed.*, vol. 82, no. 3, pp. 248–257, Jun. 2006.
[20] J.-W. Lin, J.-J. Hwang, L.-Y. Lin, and J.-L. Lin, "Measuring heart rate variability with wavelet thresholds and energy components in healthy subjects and patients with congestive heart failure," *Cardiology*, vol. 106, no. 4, pp. 207–214, 2006.
[21] S. Thurner, M. C. Feurstein, and M. C. Teich, "Multiresolution wavelet analysis of heartbeat intervals discriminates healthy patients from those with cardiac pathology," *Phys. Rev. Lett.*, vol. 80, no. 7, pp. 1544–1547, Feb. 1998.
[22] P. C. Ivanov, M. G. Rosenblum, C.-K. Peng, J. Mietus, S. Havlin, H. E. Stanley, and A. L. Goldberger, "Scaling behavior of heartbeat intervals obtained by wavelet-based time-series analysis," *Nature*, vol. 383, no. 6598, pp. 323–327, Sep. 1996.
[23] D. Verlinde, F. Beckers, D. Ramaekers, and A. E. Aubert, "Wavelet decomposition analysis of heart rate variability in aerobic athletes," *Auton. Neurosci.*, vol. 90, no. 1/2, pp. 138–141, Jul. 2001.
[24] J. Hayano, A. K. Barros, A. Kamiya, N. Ohte, and F. Yasuma, "Assessment of pulse rate variability by the method of pulse–frequency demodulation," *Biomed. Eng. Online*, vol. 4, p. 62, 2005.
[25] P. S. McKinley, P. A. Shapiro, E. Bagiella, M. M. Myers, R. E. De Meersman, I. Grant, and R. P. Sloan, "Deriving heart period variability from blood pressure waveforms," *J. Appl. Physiol.*, vol. 95, no. 4, pp. 1431–1438, Oct. 2003.
[26] I. Constant, D. Laude, I. Murat, and J. L. Elghozi, "Pulse rate variability is not a surrogate for heart rate variability," *Clin. Sci. (Lond.)*, vol. 97, no. 4, pp. 391–397, Oct. 1999.
[27] Task Force of the European Society of Cardiology and the North American Society of Pacing and Electrophysiology, Circulation, "Heart rate variability: Standards of measurement, physiological interpretation, and clinical use," Circulation, vol. 93, no. 5, pp. 1043–1065, Mar. 1996.
[28] D. B. Percival and A. T. Walden, *Wavelet Methods for Time-Series Analysis*. Cambridge, U.K.: Cambridge Univ. Press, 2000.
[29] S. Ahmad, M. Bolic, H. Dajani, and V. Groza, "Wavelet estimation of pulse rate variability from oscillometric blood pressure measurements," in *Proc. IEEE Int. Workshop Med. Meas. Appl.*, Cetraro, Italy, 2009, pp. 37–40.
[30] AHA Committee, "Recommendations for standardizations of leads and specifications for instruments in ECG and VCG," Circulation, vol. 52, pp. 11–251975.
[31] T. Ziemssen, J. Gasch, and H. Ruediger, "Influence of ECG sampling frequency on spectral analysis of RR intervals and baroreflex sensitivity using the EUROBAVAR data set," *J. Clin. Monit. Comput.*, vol. 22, no. 2, pp. 159–168, Apr. 2008.
[32] A. M. Bianchi, L. Mainardi, E. Petrucci, M. G. Signorini, M. Mainardi, and S. Cerutti, "Time-variant power spectrum analysis for the detection of transient episodes in HRV signal," *IEEE Trans. Biomed. Eng.*, vol. 40, no. 2, pp. 136–144, Feb. 1993.
[33] M. Merri, D. C. Farden, J. G. Mottley, and E. L Titlebaum, "Sampling frequency of the electrocardiogram for spectral analysis of the heart rate variability," *IEEE Trans. Biomed. Eng.*, vol. 37, no. 1, pp. 99–106, Jan. 1990.
[34] J. S. Wu, Y. C. Yang, T. S. Lin, Y.-H. Huang, J.-J. Chen, F.-H. Lu, C.-H. Wu, and C.-J. Chang, "Epidemiological evidence of altered

cardiac autonomic function in subjects with impaired glucose tolerance, but not isolated impaired fasting glucose," *J. Clin. Endocrinol. Metabolism*, vol. 92, pp. 3885–3889, 2007.

[35] J. J. de Hartog, T. Lanki, K. L. Timonen, G. Hoek, N. A. Janssen, A. Ibald-Mulli, A. Peters, J. Heinrich, T. H. Tarkiainen, R. van Grieken, J. H. van Wijnen, B. Brunekreef, and J. Pekkanen, "Associations between $PM_{2.5}$ and heart rate variability are modified by particle composition and beta-blocker use in patients with coronary heart disease," *Environ. Health Perspect.*, vol. 117, no. 1, pp. 105–111, Jan. 2009.

[36] C. H. Chen, E. Nevo, B. Fetics, P. H. Pak, F. C. P. Yin, W. L. Maughan, and D. A. Kass, "Estimation of central aortic pressure waveform by mathematical transformation of radial tonometry pressure," *Circulation*, vol. 95, pp. 1827–1836, 1997.

[37] H. Sorvoja, R. Myllylä, P. Kärjä-koskenkari, J. Koskenkari, M. Lilja, and Y. A. Kesäniemi, "Accuracy comparison of oscillometric and electronic palpation blood pressure measuring methods using intra-arterial method as a reference," *Molec. Quantum Acoust.*, vol. 26, pp. 235–260, 2005.

[38] C. E. Shannon, "Communication in the presence of noise," *Proc. IEEE*, vol. 86, no. 2, pp. 447–457, Feb. 1998.

[39] P. Li, S. H. Sur, R. E. Mistlberger, and M. Morris, "Circadian blood pressure and heart rate rhythms in mice," *Amer. J. Physiol. Reg. Integr. Comp. Physiol.*, vol. 276, no. 2, pp. 500–504, Feb. 1999.

[40] *Manual, Electronic, or Automated Sphygmomanometers*, American National Standard ANSI/AAMI SP10:2002, 2003.

[41] R. N. Bracewell, *Fourier Transform and Its Applications*. New York: McGraw-Hill, 2000.

[42] Y. Meyer, *Wavelets: Algorithms and Applications*. Philadelphia, PA: SIAM, 1993.

[43] S. Mallat, "A theory for multiresolution signal decomposition: The wavelet representation," *IEEE Trans. Pattern Anal. Mach. Intell.*, vol. 11, no. 7, pp. 674–693, Jul. 1989.

[44] I. Daubechies, *Ten Lectures on Wavelets*. Philadelphia, PA: SIAM, 1992.

[45] A. J. E. Seely and P. T. Macklem, "Complex systems and the technology of variability analysis," *Crit. Care*, vol. 8, no. 6, pp. 367–384, Dec. 2004.

[46] A. Voss, S. Schulz, R. Schroeder, M. Baumert, and P. Caminal, "Methods derived from nonlinear dynamics for analysing heart rate variability," *Philos. Trans. Roy. Soc. London A: Math. Phys. Sci.*, vol. 367, no. 1887, pp. 277–296, Jan. 2009.

[47] P. Dadelszen, M. P. Ornstein, S. B. Bull, A. G. Logan, G. Koren, and L. A. Magee, "Fall in mean arterial pressure and fetal growth restriction in pregnancy hypertension: A meta-analysis," *Lancet*, vol. 355, no. 9198, pp. 87–92, Jan. 2000.

Miodrag Bolic (M'04–SM'08) received the B.Sc. and M.Sc. degrees in electrical engineering from the University of Belgrade, Belgrade, Serbia, in 1996 and 2001, respectively, and the Ph.D. degree in electrical engineering from the State University of New York at Stony Brook in 2004.

He is the Director of the Radio Frequency Identification Systems Laboratory and the Computer Architecture Research Group, University of Ottawa, Ottawa, ON, Canada. He is currently an Associate Professor with the School of Information Technology and Engineering, University of Ottawa. He has more than seven years of industrial experience related to embedded system design and signal processing. He has published more than 60 journal papers and conference proceedings. His research interests include computer architectures, hardware accelerators, signal processing for biomedical applications, and RFID.

Hilmi Dajani (M'07) received the B.Eng. degree in electrical engineering from McMaster University, Hamilton, ON, Canada, in 1987 and the M.Sc. and Ph.D. (collaborative program in biomedical engineering) degrees in electrical and computer engineering from the University of Toronto, Toronto, ON, Canada, in 1991 and 2004, respectively.

He is currently an Assistant Professor with the School of Information Technology and Engineering, University of Ottawa, Ottawa, ON, Canada. He has several years of experience in implementing technical projects in a hospital setting and in the biomedical technology industry. He has also conducted research on auditory-inspired speech processing, speech-evoked potentials, and speech production with modified auditory feedback. His research interests include the development of new methods for the analysis of cardiorespiratory function and the development of instrumentation for the assessment and treatment of speech and hearing impairments.

Saif Ahmad received the B.Eng. degree in electrical engineering from Aligarh Muslim University, Aligarh, India, in 1996, the M.Sc. degree in computer science from the University of Birmingham, Birmingham, U.K., in 2001, and the Ph.D. degree in computer science from the University of Surrey, Guildford, U.K., in 2007.

He is currently a Research Associate in the School of Information Technology and Engineering at the University of Ottawa, Canada. Previously he was a Postdoctoral Fellow in the Divisions of Thoracic Surgery and Critical Care Medicine at the University of Ottawa, Canada. Additionally, he has over three years of industrial experience related to high voltage engineering, electrical power generation and distribution, and electrical machines at Tata Chemicals Ltd., India. In 2009, his work on heart rate variability analysis for the diagnosis, prognosis, and prediction of sepsis was published in the Public Library of Science (PLoS) One and Critical Care. This work was also accorded prominent coverage by the Ottawa Citizen. He has published more than 13 papers in peer-reviewed journals and conference proceedings. His major research interests include biomedical signal processing and financial time-series analysis.

Dr. Ahmad has served as a Reviewer for several IEEE and medical journals and conference proceedings.

Voicu Groza (M'97–SM'02) received the Dipl.Eng. degree in computer engineering and the Dr.Eng. degree in electrical engineering from the Polytechnic Institute of Timisoara, Timisoara, Romania, in 1972 and 1985, respectively.

He was a Professor with the Polytechnic University of Timisoara. In 1997, he joined the University of Ottawa, Ottawa, ON, Canada, where he is currently with the School of Information Technology and Engineering. He is the author or a coauthor of more than 150 technical papers. His research interests include biomedical instrumentation and measurement, and reconfigurable computers.

Dr. Groza has served as a Conference or Technical Program Chair at several major international events such as the IEEE International Workshop on Medical Measurement and Applications (MeMeA 2008–2010), the 2005 IEEE International Conference on Instrumentation and Measurement (IMTC 2005), and the 2006 IEEE Canadian Conference on Electrical and Computer Engineering (CCECE 2006). He is currently the Chair of the IEEE Working Group on Standard for Objective Measurement of Systemic Arterial Blood Pressure in Humans.

Izmail Batkin received the M.S. and Ph.D. degrees in theoretical physics from the Voronezh State University, Voronezh, Russia, in 1965 and 1969, respectively, and the Dr.Sci. degree in nuclear physics from the Leningrad State University, St. Petersburg, Russia, in 1982.

He is a Chief Scientist with Biopeak Corporation, Ottawa, ON, Canada. Prior to this, he was a Professor with the Voronezh State University and an Adjunct Professor with Carleton University, Ottawa, ON, Canada. He is currently a Research Consultant with the Ottawa Hospital and with the School of Information Technology and Engineering, University of Ottawa, Ottawa, ON, Canada. He has been involved in the successful development and testing of a new generation of wearable physiological electrodes and monitors for the home and clinical environments. He is the holder of one patent and has published more than 150 refereed papers, many in top-notch journals such as *Physical Review, Journal of Physics*, and the *Soviet Journal of Nuclear Physics*. His major research interests include theoretical and nuclear physics and medical physics. Over the years, his research has focused on noninvasive monitoring of physiological parameters.

Sreeraman Rajan (M'90–SM'06) received the B.E. degree in electronics and communications from Bharathiyar University, Coimbatore, India, in 1987, the M.Sc. degree in electrical engineering from Tulane University, New Orleans, LA, in 1990, and the Ph.D. degree in electrical and computer engineering from the University of New Brunswick, Fredericton, NB, Canada, in 2004.

From 1986 to 1990, he was a Scientific Officer with the Reactor Control Division, Bhabha Atomic Research Center, Bombay, India, where he was involved in the control, safety, and regulation of nuclear research and power reactors. From 1997 to 1998, in addition to various jobs, he carried out research funded by a grant from Siemens Corporate Research, USA. From 1999 to 2000, he worked on optical components and the development of signal processing algorithms for advanced fiber optic modules with JDS Uniphase. From 2000 to 2003, he was with Ceyba Corporation, where he was involved in channel monitoring, dynamic equalization, and control of optical power for advanced fiber optical communication systems. In 2004, he was with Biopeak Corporation, where he developed signal processing algorithms for noninvasive medical devices. Since December 2004, he has been with Defence Research and Development Canada, Ottawa, ON, as a Defence Scientist. He has published several journal papers and conference proceedings. He is the holder of one patent and has two disclosures of invention to his credit. His research interests include signal processing, biomedical signal processing, communications, and pattern classification.

Dr. Rajan is a member of the Eta Kappa Nu Honor Society. He is currently the Vice Chair of the IEEE Ottawa Section and the Chair of the Ottawa Chapter of the IEEE Engineering in Medicine and Biology Society (EMBS). He has been involved with several IEEE conferences in various capacities. He has served as a Reviewer for several IEEE Transactions and conferences.